FLUKA-BASED OPTIMIZATION OF PION PRODUCTION FOR A MUON COLLIDER DEMONSTRATOR

R. Alharthy*[1], S. Dasu[1], Ch.-H. Nee[1], P. Rao[1], C. Vuosalo[1],
J. Eldred[2], M. Hedges[2], S. Jindariani[2], D. Stratakis[2], K. Yonehara[2]
[1]University of Wisconsin–Madison, Madison, WI, USA
[2]Fermi National Accelerator Laboratory, Batavia, IL, USA

Abstract

This study uses FLUKA simulations to investigate pion production from proton interactions with a graphite target for muon collider applications. A 40 cm target is struck with 0.8 GeV and 8 GeV/c proton beams, and pion yields are evaluated in terms of angular and energy distributions. The dependence of pion yield on target length is also examined, showing saturation near one interaction length for the 0.8 GeV beam, and saturation near two interaction lengths for the 8 GeV/c beam. In addition to total production, a subset of "acceptable" pions is defined based on capture constraints (kinetic energy <400 MeV, forward-going, and escaping the target). The results show that while the 8 GeV/c beam produces higher overall yields, the 0.8 GeV beam provides a larger fraction of pions within the desired constraints. Charge asymmetry is also observed in pion production.

INTRODUCTION

The development of a future muon collider represents a promising path toward probing physics at the energy frontier. A central challenge in realizing such a facility lies in the efficient production of high-intensity muon beams. Since muons are obtained from the decay of charged pions $\pi^{\pm} \rightarrow \mu^{\pm} + \nu$, optimizing pion production at the target station is a critical component of the collider design.

A demonstrator of a muon production system from target to final cooling is needed to make a convincing case for committing to build a muon collider. We investigate the design challenges and site specific optimization of the target system for a demonstrator at FNAL. Pion production is governed by the interaction of a high-energy proton beam with a dense target material, typically via inelastic proton–nucleus collisions. The resulting pion yield depends on several competing factors, including the incident proton beam energy, target material, and geometric parameters such as target length and radius. In addition to total yield, analyzing the energy spectrum and angular distribution of pions plays a crucial role in determining downstream design and efficiency of the capture and transport system.

A key consideration in target optimization is the proton beam energy. Higher energies increase the inelastic proton–nucleus cross section, producing higher pion multiplicities with a stronger forward boost, improving capture efficiency. Beam energies around 8 GeV are therefore commonly used as a reference for both demonstrator and collider-scale studies [1], and are broadly comparable to the 5 GeV-10 GeV proton driver scenarios considered in the Muon Collider 2026 European Strategy update [2].

Lower-energy beams, however, are particularly relevant for a muon ionization cooling demonstrator. Proton energies near 0.8 GeV, such as those foreseen in [3], are not intended for a collider but offer a practical and cost-effective option for a near-term demonstrator [1]. Leveraging existing or planned high-intensity proton infrastructure at Fermilab [4] could further reduce the need for a dedicated high-energy driver.

In this work, we compare pion production from 0.8 GeV and 8 GeV/c proton beams on candidate targets using FLUKA simulations [5, 6]. The 8 GeV/c case represents both demonstrator and collider scenarios, while 0.8 GeV is primarily motivated by demonstrator studies. We evaluate total pion yields and the kinematic distributions relevant for capture, assessing whether lower-energy, high-intensity beams can provide a viable front-end for a muon collider demonstrator.

SIMULATION SETUP

The simulation geometry consists of a graphite target aligned along the beam axis. The target has a length of 40 cm (approximately one interaction length for graphite) and a radius of 0.15 cm. The relatively small radius is chosen to reduce reabsorption and secondary interactions of produced pions, thereby improving pion yield for the demonstrator. A proton beam containing 100,000 primaries is initialized 20 cm upstream of the target, propagating in vacuum.

The primary objective of this study is to characterize pion production within the target for proton beams of different energies. One key observable is the angular distribution of the produced pions. To preserve the intrinsic production kinematics, no magnetic field is included in the simulation.

In selected studies, a comparison is made between pions produced within the target and those that escape it. Escaping pions are recorded by tracking particles crossing the target–vacuum boundary. A custom user routine was developed to register only the first occurrence of each particle. This approach enables the extraction of pion production distributions within the target.

* ralharthy@wisc.edu

PION SELECTION CRITERIA

In a muon collider, a proton beam strikes a target to produce secondary pions, which decay into muons. While pion production spans a wide range of energies and angles, the downstream solenoidal capture system can only efficiently accept a limited range, constrained by the magnetic field and aperture.

Design studies indicate that pion capture is most effective for energies below 400 MeV. These considerations are consistent with the International Muon Collider Collaboration (IMCC [7]) front-end design, which targets low-energy pions.

Motivated by this, the selection criteria used in this study are:

- pions that escape the target,
- pion kinetic energy < 400 MeV,
- forward-going pions, defined by $\cos\theta_z > 0$.

These cuts select pions most relevant for efficient capture, and both positive and negative yields are evaluated to assess charge symmetry.

DEPENDENCE OF PION YIELD ON TARGET LENGTH

Before examining the detailed phase space distributions of produced pions, it is instructive to first understand how the overall yield scales with target length. Figure 1 shows the evolution of total and accepted pion production as a function of graphite target length for both 0.8 GeV and 8 GeV/c proton beams. In general, we expect pion production to level off after approximately one interaction length of graphite (around 40 cm), where the primary proton beam has largely undergone its first inelastic interactions.

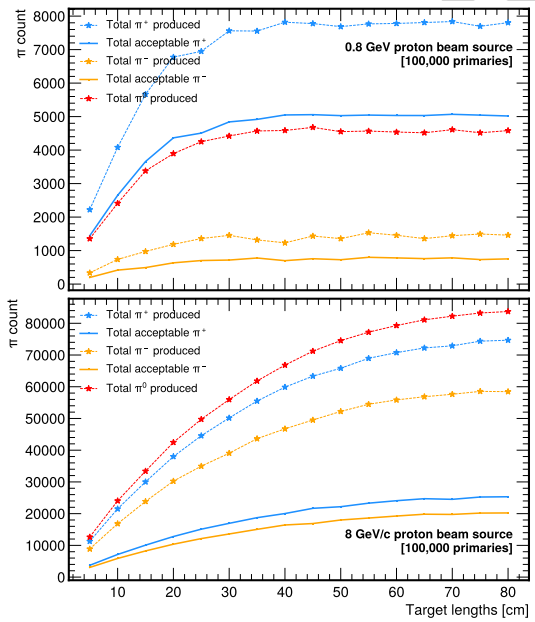

Figure 1: π yields for different target lengths of 0.8 GeV (top) and 8 GeV/c (bottom) proton beams incident on a graphite target.

This expectation holds for the 0.8 GeV beam, where the yield clearly saturates near this length. In contrast, for the 8 GeV/c beam, pion production continues to increase beyond one interaction length. This is driven by higher-energy secondary particles that retain sufficient energy to undergo further interactions with carbon nuclei, producing additional pions and extending the cascade.

These results motivate the choice of a 40 cm target for the detailed analysis that follows.

PION YIELD CHARACTERIZATION

Building on the previous sections, where the simulation framework and target configuration were established, we now turn to a quantitative characterization of pion production in a 40 cm long graphite target struck by proton beams of 0.8 GeV and 8 GeV/c. The goal is not only to compare total pion yields, but also to identify the subset of pions that are relevant for downstream capture and transport in a muon collider front-end system.

Angular Distributions

The angular distributions in Fig. 2 reveal a strong forward bias in pion production for both beam energies. This effect is significantly more pronounced for the 8 GeV/c beam, where pion production is heavily peaked near $\cos\theta_z \approx 1$. In contrast, the 0.8 GeV beam produces a broader angular spread, with a comparatively larger fraction of pions at lower $\cos\theta_z$. However, after applying the acceptance criteria, both cases show a substantial reduction in yield, particularly at large angles, reinforcing the importance of forward-focused production for efficient capture.

Energy Distributions

The pion kinetic energy spectra in Fig. 3 further highlight the differences between the two beam energies. The 0.8 GeV beam produces pions predominantly in the low-energy region, with a significant fraction naturally lying below the 400 MeV threshold. As a result, a relatively larger proportion of produced pions satisfy the energy acceptance criterion.

On the other hand, the 8 GeV/c beam generates a much broader energy spectrum extending to several GeV. While the total pion yield is considerably higher, only a small fraction falls below the 400 MeV range relevant for capture. This demonstrates a key trade-off: higher beam energy increases total production but reduces the fraction of usable pions within the desired kinematic region.

One important feature seen in both Fig. 2 and Fig. 3 is the asymmetry between π^+ and π^- production, which is more pronounced at 0.8 GeV. In this regime, single-pion production processes dominate, favoring π^+. In contrast, at 8 GeV/c, multi-pion production becomes dominant, leading to a more balanced yield of π^+ and π^-.

Angular-Energy Correlations

The two-dimensional angular–energy distributions provide deeper insight into the phase space structure for pions

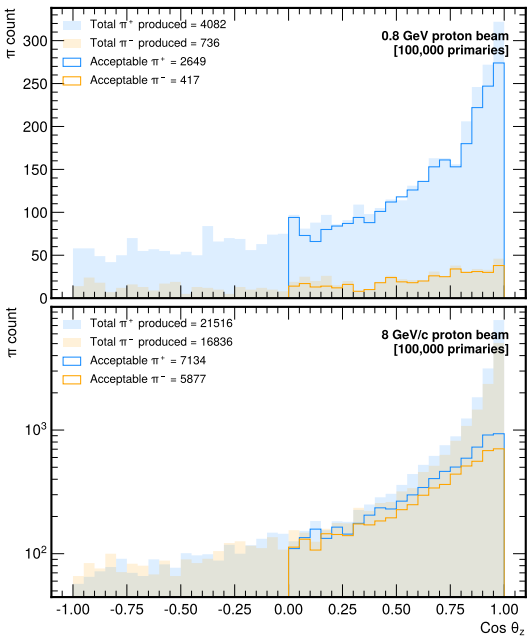

Figure 2: Angular distributions for pions produced by 0.8 GeV (top) and 8 GeV/c (bottom) proton beams incident on a graphite target. Note that the top panel is shown on a linear y-scale, while the bottom panel is shown on a logarithmic y-scale. The bin size for both plots is $\Delta(\cos\theta_z) = 0.05$.

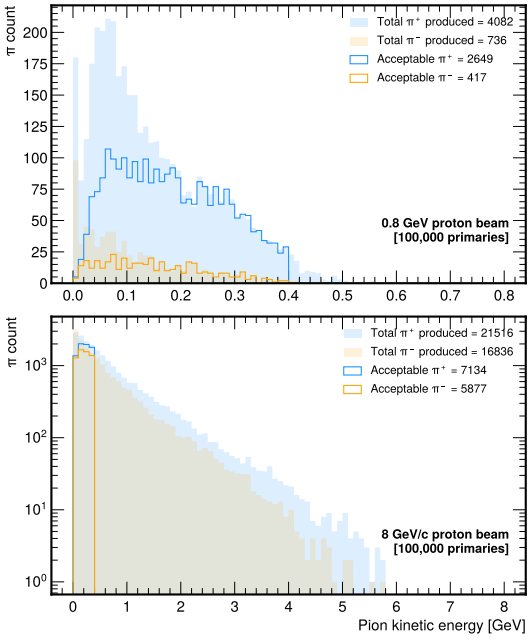

Figure 3: Energy distributions for pions produced by 0.8 GeV (top) and 8 GeV/c (bottom) proton beams incident on a graphite target. Note that the top panel is shown on a linear y-scale, while the bottom panel is shown on a logarithmic y-scale. The bin size for the top plot is 0.01 GeV and for the bottom plot is 0.1 GeV

that have passed the selection criteria. For the 0.8 GeV beam, Fig. 4, the population of pions is concentrated at low energies and spans a relatively wide angular range, though the highest densities remain in the forward direction.

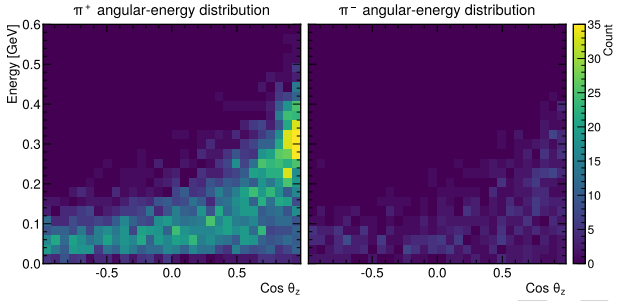

Figure 4: Angular-Energy distributions for pions produced by 0.8 GeV proton beam incident on a graphite target.

In contrast, the 8 GeV/c beam, Fig. 5, exhibits a strong concentration of pions at high $\cos\theta_z$, with a clear correlation between forward emission and higher energies. The acceptable pion population is confined to a narrow band at low energies and near-forward angles, indicating that only a small, well-defined region of the produced phase space contributes to potentially usable yield.

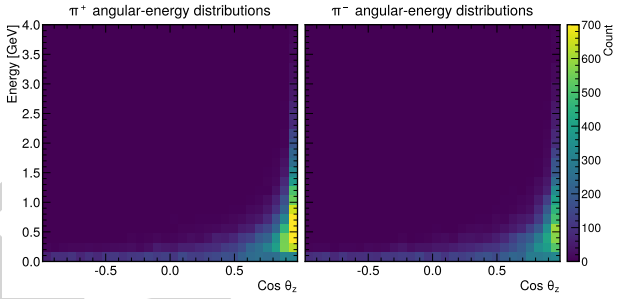

Figure 5: Angular-Energy distributions for pions produced by 8 GeV/c proton beam incident on a graphite target.

CONCLUSION

These results show that optimization of a target system for a muon collider depends not only on pion yield, but also on beam intensity and downstream acceptance. Although higher-energy proton beams produce more pions per interaction, Fermilab can provide roughly two orders of magnitude more 0.8 GeV protons than 8 GeV/c protons. Consequently, the lower-energy beam can produce a larger overall yield of useful positive pions at lower operational cost, despite its lower per-event production rate.

Since the primary goal of the demonstrator is to validate ionization cooling, demonstrating the concept with π^+-derived muons is sufficient, as the cooling performance is expected to be symmetric for positive and negative muons. In addition, previous studies on the influence of target geometry on pion and muon production [8] further emphasize the importance of jointly optimizing beam and target parameters for future muon collider applications.

REFERENCES

[1] C. Rogers, "A demonstrator for muon ionisation cooling", *Phys. Sci. Forum*, vol. 8, no. 1, p. 37, 2023. doi:10.3390/psf2023008037

[2] A. Abdelhamid *et al.*, "United States muon collider community white paper for the European Strategy for particle physics update", *arXiv*, Mar. 2025. doi:10.48550/arXiv.2503.23695

[3] M. Ball *et al.*, "The PIP-II conceptual design report", Fermi National Accelerator Laboratory, Batavia, IL, USA, Reps. FERMILAB-DESIGN-2017-01 FERMILAB-TM-2649-AD-APC, Mar. 2017. doi:10.2172/1346823

[4] M. J. Syphers, "Fermilab proton beam for Mu2e", *AIP Conf. Proc.*, vol. 1222, no. 1, pp. 391–395, Mar. 2010. doi:10.1063/1.3399350

[5] T. Böhlen *et al.*, "The FLUKA code: developments and challenges for high energy and medical applications", *Nucl. Data Sheets*, vol. 120, pp. 211–214, 2014. doi:10.1016/j.nds.2014.07.049

[6] A. Fasso, A. Ferrari, J. Ranft, and P. R. Sala, "FLUKA: a multi-particle transport code", CERN, Geneva, Switzerland, Rep. CERN-2005-10, Rep., 2005. doi:10.2172/877507

[7] C. Accettura *et al.*, "Interim report for the International Muon Collider Collaboration (IMCC)", *arXiv*, Jul. 2024. doi:10.48550/arXiv.2407.12450

[8] R. Al-Harthy, "FLUKA-based optimization of muon production target design for a muon collider demonstrator", *arXiv*, Feb. 2026. doi:10.48550/arXiv.2602.16672